H1prelim-08-032 Submitted to

XVI International Workshop on Deep-Inelastic Scattering, DIS2008, April 7-11, 2008, London
Parallel Session **Hadronic Final States and QCD**

Electronic Access:https://www-h1.desy.de/publications/H1preliminary.short_list.html

Measurement of Inclusive Jet Production Deep-Inelastic ep Scattering at low Q^2

H1 Collaboration

Abstract

Jet production is studied in deep-inelastic positron-proton scattering over a range of four momentum transfer squared $5 < Q^2 < 100$ GeV^2. The data were taken with the H1 detector at HERA in the years 1999-2000 and correspond to integrated luminosity of 43.5 pb^{-1}. Jets are defined in the Breit frame with the inclusive k_T algorithm and have a minimum transverse momentum of 5 GeV. Inclusive jet cross sections are measured differentially in Q^2 and E_T of the jets and compared to the predictions of perturbative QCD calculations in next-to-leading order of the strong coupling constant α_s. The strong coupling α_s is extracted from this measurement.

1 Introduction

This paper presents measurements of inclusive multijet cross-sections in the Breit frame at low Q^2 values ($5 < Q^2 < 100\ \mathrm{GeV}^2$). Jets are identified with the inclusive k_t algorithm in the Breit frame of reference.

The data sample analysed is collected in 1999-2000, and corresponds to an integrated luminosity of $43.5pb^{-1}$. Compared to previous H1 publications [2, 3] this corresponds to twice the statistics and in addition the systematic errors have been reduced. The total center of mass energy $\sqrt{s}$ is slighly higher in the new data (320 GeV compared to 300 GeV) due to higher proton beam energy (920 GeV compared to 820 GeV). The results on inclusive jet production are presented in both single differential cross sections as a function of Q^2 and E_T, respectively, and in double differential cross sections in these variables.

2 Event Kinematics and Reconstruction

The kinematic range of this analysis is defined by $5 < Q^2 < 100\ \mathrm{GeV}^2$ and $0.2 < y < 0.7$. The kinematic variables x, Q^2 and y are determined using the information from scattered electron and the hadronic final states ($e - \Sigma - method$) [1].

Jets are defined using the inclusive k_t cluster algorithm in the Breit frame in which the virtual photon and the parton collide head on. In this frame the transverse energies of jets are closely related to transverse energies of partons emerging the hard scattering. Jets are selected by requiring the transverse energy to be larger than 5 GeV.

3 Event selection

The analysis use the data sample collected in positron-proton interactions in 1999-2000. Events were triggered by combinations of SPACAL electron and track triggers. The trigger efficiency for jet events is close to 100%. The total integrated luminosity of data sample is $43.5pb^{-1}$. Further cuts are applied to ensure the quality of data and remove non-DIS events: the event vertex is required to be within 35 cm from the nominal vertex, energy and angle of scattered electron to be $E_e > 7.5\ GeV$, $156^\circ < \theta_e < 175^\circ$, respectively.

Jets are identified with the inclusive k_t algorithm in Breit frame. The minimum E_T is required to be above 5 GeV in that frame. To ensure that jets are fully contained in the calorimeter, the pseudorapidity of jets in the laboratory frame is required to be $-1 < \eta^{Lab} < 2.5$.

The final data sample contains 175,000 events with at least one jet satisfying the selection criteria.

4 Monte Carlo Models and Correction procedure

For the the calculation of correction factors due to detector effects, initial state radiation and hadronization RAPGAP3.1 and DJANGOh1.4 Monte Carlo generators are used. The CTEQ6D and CTEQ6L parametrizations of the parton distribution functions in the proton are used in RAPGAP and DJANGOh, respectively.

The data distributions are corrected for effects of limited detector acceptance and resolution and for higher order QED effects using bin-to-bin corrections. The bin sizes were chosen to ensure the sufficient statistics and sufficiently high stability and purity in each bin.

The correction factor for each distribution are defined as the ratio of cross section at hadron level for Monte Carlo sample which is generated without QED corrections to that at detector level with QED corrections included. The correction factor is taken as the average of the values from DJANGO and RAPGAP, respectively. The difference between the of corrections from the two Monte Carlo programs is on the average less than 5% and is included in the systematic erros.

For comparison with NLO calculations the hadronization corrections are calculated as the ratios of cross sections on the parton level to that on the hadron level. Again, the average of the corrections obtained from the two Monte Carlo programs is taken as the final correction factor. The hadronization correction factors agree on the level of 2% between the two Monte Carlo simulations.

5 Systematic Uncertainties

The following sources of systematic errors are considered:

- the 2% uncertainty on the absolute hadronic energy scale of the LAr calorimeter leads to an uncertainty of about 4–10% on the jet cross section. This is strongly correlated between data points;
- the uncertainty of the SPACAL hadronic energy scale of 7% contributes to less than 1% to the cross section;
- the uncertainties on the measurements of the positron energy (2%) and angle (1mrad) lead to 1–3% systematic uncertainties in the cross sections;
- the uncertainty of the corrections for detector effects and initial state radiation is 2–15%,
- luminosity is measured with the uncertainty of 1.5%;
- finally, 1% uncertainty is attributed to the trigger efficiencies as evaluated using independent triggers.

6 Results

The results shown in figires 1-5 comprise inclusive jet cross sections as function of Q^2 and E_T, as well as the double differential cross sections in Q^2 and E_T.

The measured cross-sections are compared with NLO QCD calculations. The NLO calculations are made using the NLOJET++ program. The calculations are performed in the $\overline{\mathrm{MS}}$ scheme for five massive quark flavours, and the parton PDF of the proton taken from the CTEQ6 set [5]. Q^2 is used as factorization scale (μ_F), whereas the renormalization scale (μ_R) is chosen to be $\sqrt{(Q^2 + E_T^2)/4}$. The error band on NLO predictions reflect the variation the scales μ by a factor of 2 up and down using the NLOJET++ [6] program. The NLO QCD calculations corrected for hadronization provide quite reasonable description of single inclusive jet cross sections. The measurements show strong sensitivity to the choice of the renormalisation scale. The calculations have been repeated with $\mu_R = E_T$. This scale provides worse description of the data at lower Q^2 and E_T, as shown in the figures 3 and 4.

The fastNLO program [4] was used to estimate uncertainty on NLO predictions arising from variations of factorization and renormalization scales, from the value of α_s and the proton PDF. The different sources of uncertainties are shown with different error bands:

- uncertainty arising from the renormalisation and factorisation scales (μ_R, μ_F) are estimated by varying them by factors 2 and 0.5 separately and added the results of variation in quadrature. The contribution to uncertainty is up to 30%.
- variation of α_s between 0.116 and 0.120 gives variation of cross sections up to 5%
- variation of 40 different eigenvectors of CTEQ6 proton PDF parameterisation gives up to 6% incertainty

7 Extraction of the strong coupling α_s

The measured double differential inclusive jet cross sections (Fig.5) have been used to extract the strong coupling α_s. The extracted value of $\alpha_s(M_Z)$ averaged over all measured data points is

$$\alpha_s(M_Z) = 0.1186 \pm 0.0014(exp)^{+0.0132}_{-0.0101}(theory) \pm 0.0021(pdf), \;\; \chi^2/ndf = 20.49/27$$

The results of the fit are shown in Figs.7 and Figs.8. Fig.9 shows the $\alpha_s(\mu = Q)$ from this measurement together with the values obtained from high Q^2 region ($Q^2 > 150\ GeV^2$) [7].

8 Summary

Inclusive jet cross-sections have been measured for values of Q^2 between 5 and 100 GeV^2 and $0.2 < y < 0.7$ with the H1 detector. Jets were selected using the inclusive k_T algorithm in the Breit frame and were required to have a minimum transverse energy of $5\ \mathrm{GeV}$. QCD calculations up to second order in the strong coupling constant α_s were compared with the data.

The statistcal precision in the present measurement is on the level of 0.5-0.7$\%$ for the single differential jet cross sections, and 3-4$\%$ for the double differential cross sections.

The value of strong coupling α_s is extacted from the measurements.

References

[1] U. Bassler, G. Bernardi, ”On the kinematic reconstruction of deep inelastic scattering at HERA: The Sigma method”, DESY-94-231, *Nucl. Instrum. Methods* **A 361**, 197 (1995), [hep-ex/9412004].

[2] C. Adloff *et al.* [H1 Collaboration], ”Measurement and QCD Analysis of Jet Cross Sections in Deep-Inelastic Positron-Proton Collisions at $\sqrt{s}$ of 300 GeV”, *Eur. Phys. J.* **C 19**, 289 (2001), [hep-ex/0010054];

[3] C. Adloff *et al.* [H1 Collaboration], ”Measurement of Inclusive Jet Cross-Sections in Deep-Inelastic ep-Scattering at HERA”, *Phys. Lett.* **B 542**, 19 (2002), [hep-ex/0206029];

[4] T.Kluge, K.Rabbertz and M.Wobish, ”fastNLO: Fast pQCD calculations for PDF fits.” [hep-ph/0609285];
T.Kluge, private communication

[5] D. Stump *et al.*, ” Inclusive jet production, parton distributions, and the search for new physics”, *JHEP 0310:046,2003.*

[6] Z. Nagy, Z. Trocsanyi, *Phys. Rev. Lett.* **87**, 082001 (2001), [hep-ph/0104315].

[7] Inclusive Jet Production at high Q^2 and determination of α_s, H1preliminary-08-031, (*https://www-h1.desy.de/h1/www/publications/htmlsplit/H1prelim-08-031.long.html*)

Measurement	$\alpha_S(M_Z)$	exp.error	scale error		PDF error	χ^2/ndf
$\sigma_{Incl.JET} = f(Q^2, E_T)$ (low Q^2)	0.1186	0.0014	+0.0132	-0.0101	0.0021	20.5/27
$\sigma_{Incl.JET}/\sigma_{DIS}, \sigma_{2JET}/\sigma_{DIS}$, $\sigma_{3JET}/\sigma_{DIS}$ (high Q^2)	0.1182	0.0008	+0.0041	-0.0031	0.0018	54.8/53

Table 1: Values of $\alpha_S(M_Z)$ obtained from a fit of 28 measurements of double differential inclusive jet cross sections $d^2\sigma/dQ^2dE_T$ (this measurement, upper row) and from the fits to the inclusive jet, dijet and treejet normalised cross sections at high Q^2 ($Q^2 > 150\ GeV^2$) [7]

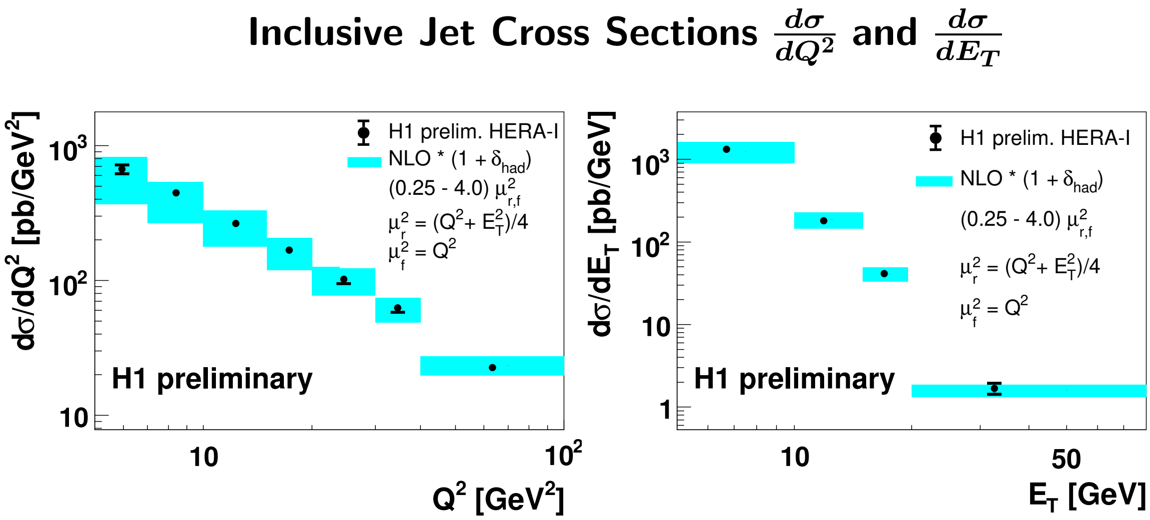

Figure 1: Inclusive jet cross sections $d\sigma/dQ^2$ and $d\sigma/dE_T$, compared with NLO predictions corrected for hadronisation. The NLO calculation use the factorization scale $\mu_F^2 = Q^2$ and the renormalization scale $\mu_R^2 = (Q^2 + E_T^2)/4$. The error bands reflect the uncertainties on NLO predictions arising from either hadronisaton corrections and the variation of renormalisation anf factorisation scales by factors 2 and 0.5.

Inclusive Jet Cross Sections $\frac{d\sigma}{dQ^2}$, $\frac{d\sigma}{dE_T}$

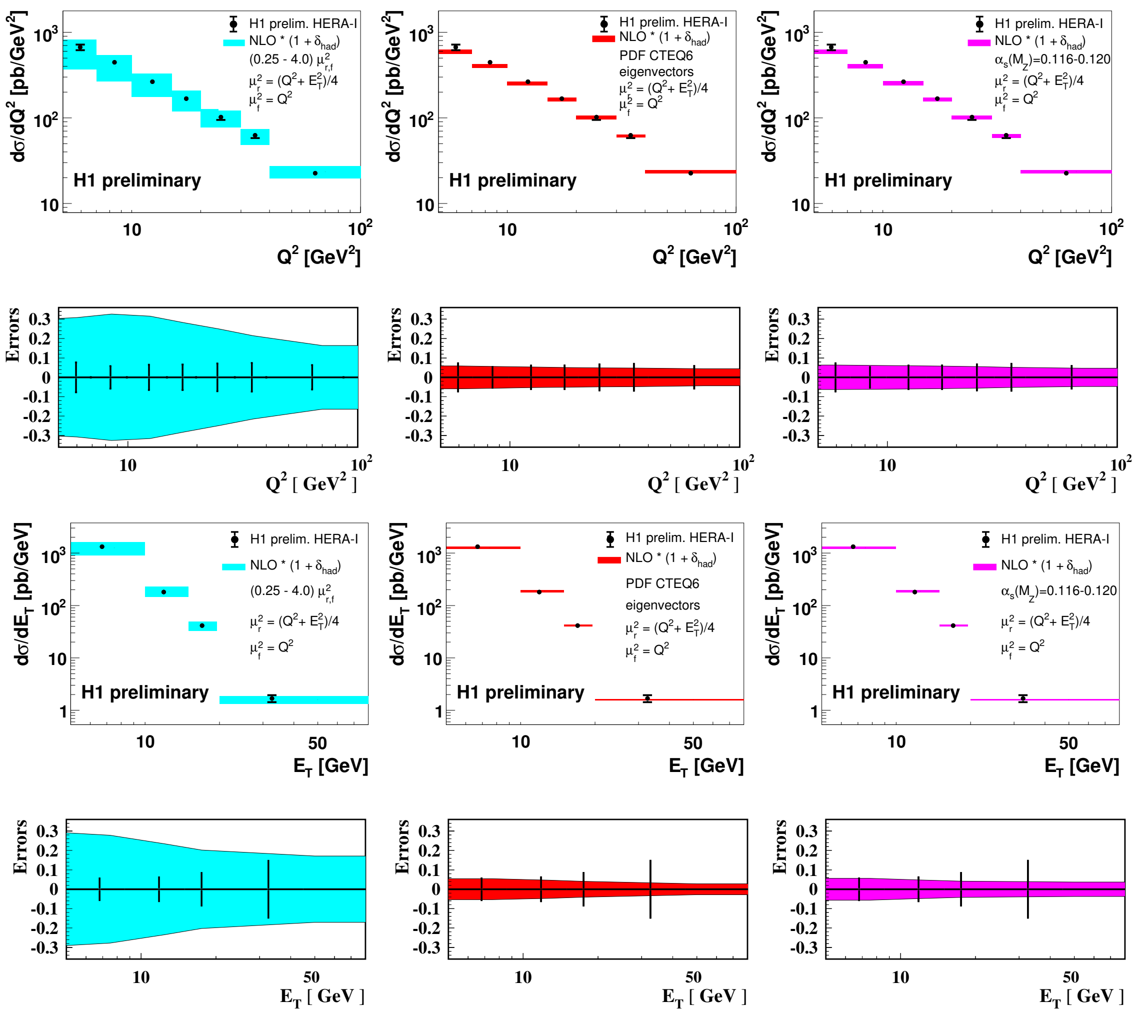

Figure 2: Inclusive jet cross sections $d\sigma/dQ^2$ and $d\sigma/dE_T$, compared with NLO predictions corrected for hadronisation. The NLO calculation use the factorization scale $\mu_F^2 = Q^2$ and the renormalization scale $\mu_R^2 = (Q^2 + E_T^2)/4$. The error bands reflect the uncertainties on NLO predictions arising from either hadronisaton corrections and the variation of renormalisation anf factorisation scales by factors 2 and 0.5, or variation of α_s from 0.116 to 0.120, or PDF uncertainties calculated from variation of 40 eigenfunctions of CTEQ6.1 proton PDF.

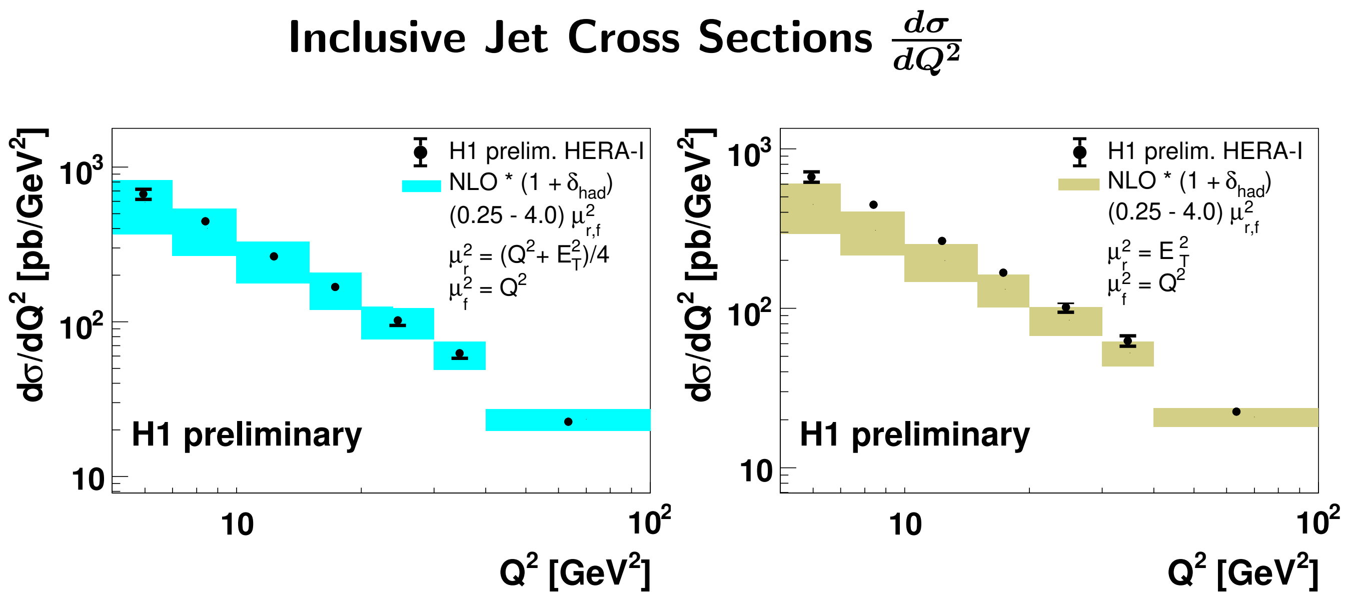

Figure 3: Inclusive jet cross sections $d\sigma/dQ^2$, compared with NLO predictions corrected for hadronisation using two different choices of renormalisation scale $\mu_R^2 = (Q^2 + E_T^2)/4$ or E_T^2.

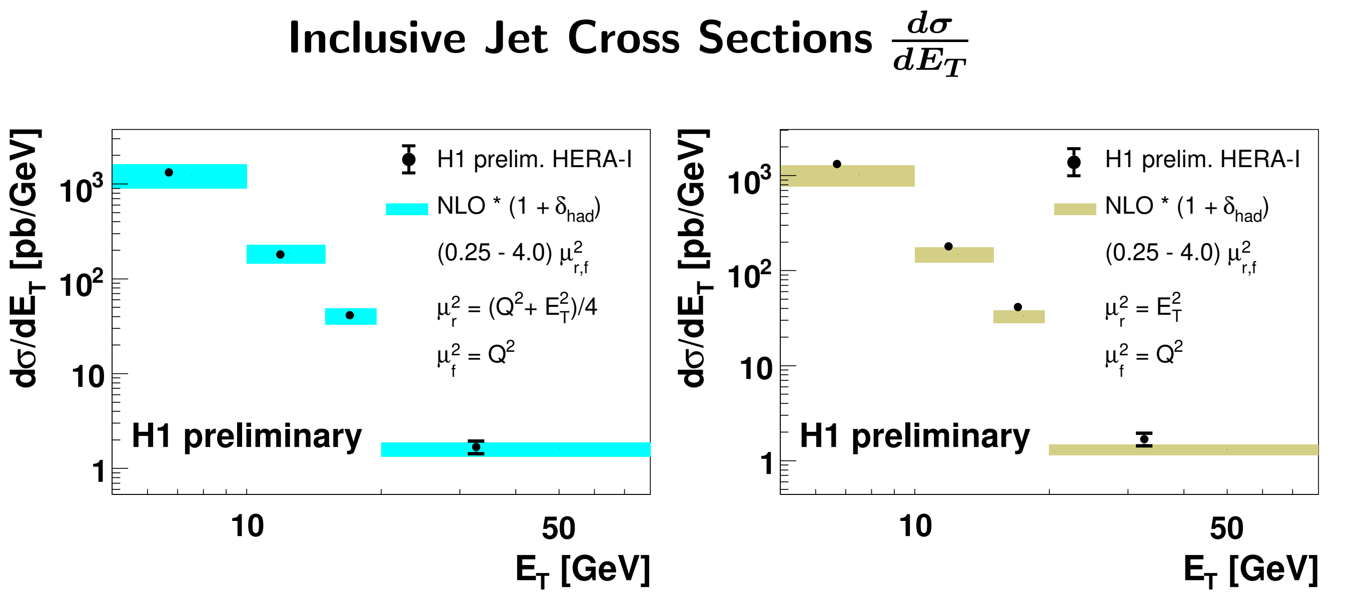

Figure 4: Inclusive jet cross sections $d\sigma/dE_T$, compared with NLO predictions corrected for hadronisation using two different choices of renormalisation scale $\mu_R^2 = (Q^2 + E_T^2)/4$ or E_T^2.

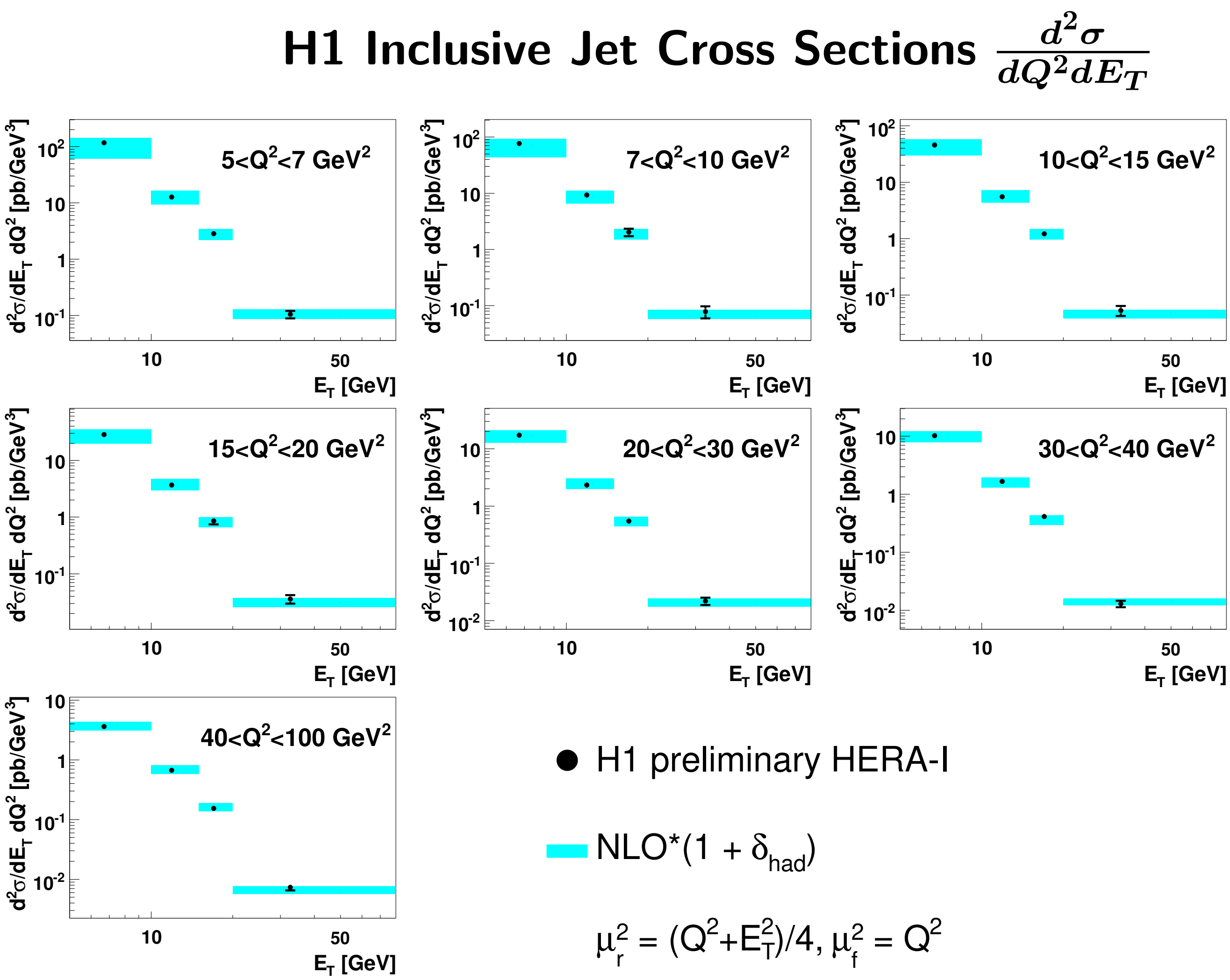

Figure 5: Inclusive double differential jet cross sections, compared with NLO predictions corrected for hadronisation. The error bands reflect the uncertainties on NLO predictions arising from hadronisation corrections and the variation of renormalisation and factorisation scales by factors 2 and 0.5 and the hadronisation. The NLO calculation use the factorization scale $\mu_F^2 = Q^2$ and the renormalization scale $\mu_R^2 = (Q^2 + E_T^2)/4$

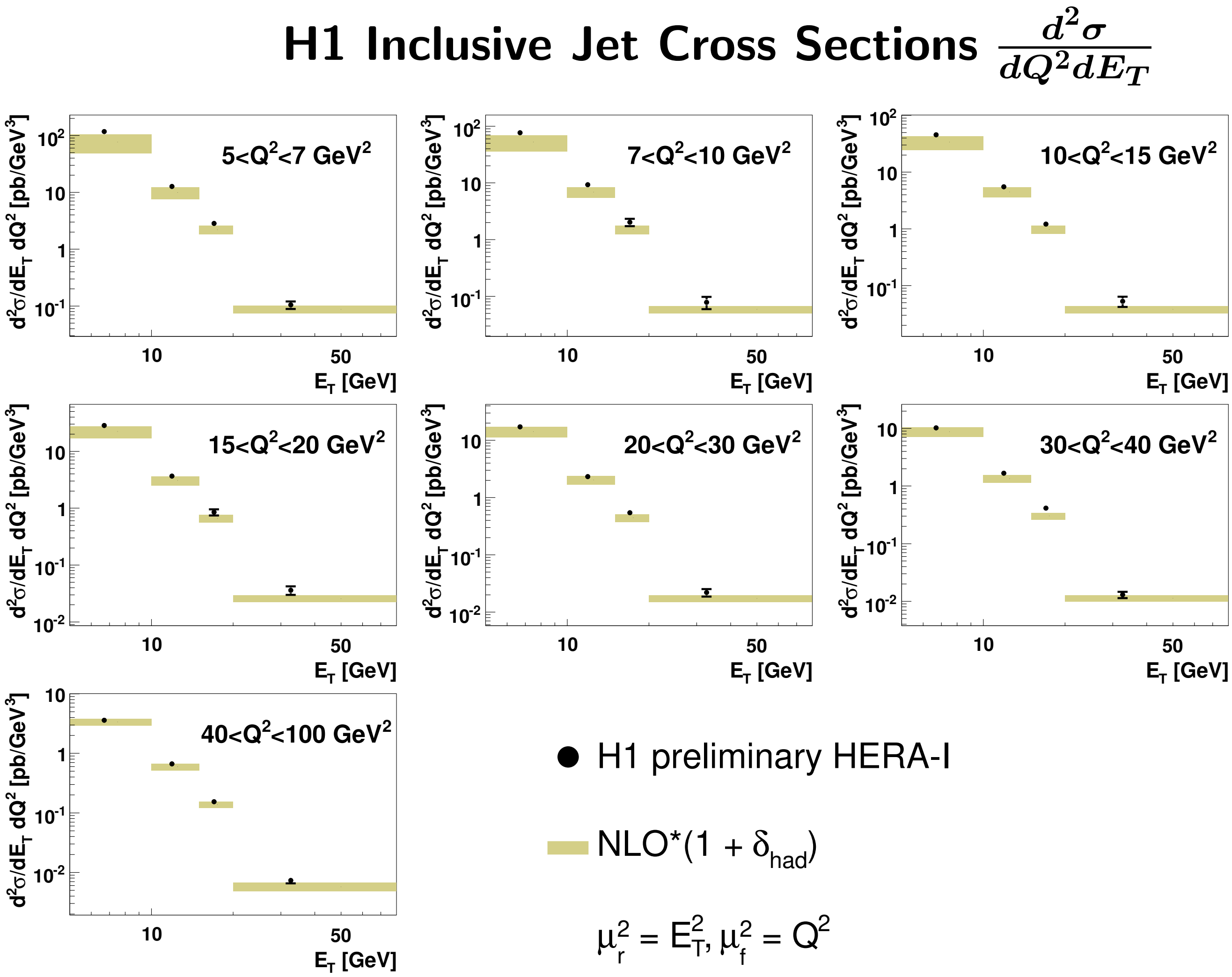

Figure 6: Inclusive double differential jet cross sections, compared with NLO predictions corrected for hadronisation. The error bands reflect the uncertainties on NLO predictions arising from hadronisation corrections and the variation of renormalisation and factorisation scales by factors 2 and 0.5 and the hadronisation. The NLO calculation use the factorization scale $\mu_F^2 = Q^2$ and the renormalization scale $\mu_R^2 = E_T^2$

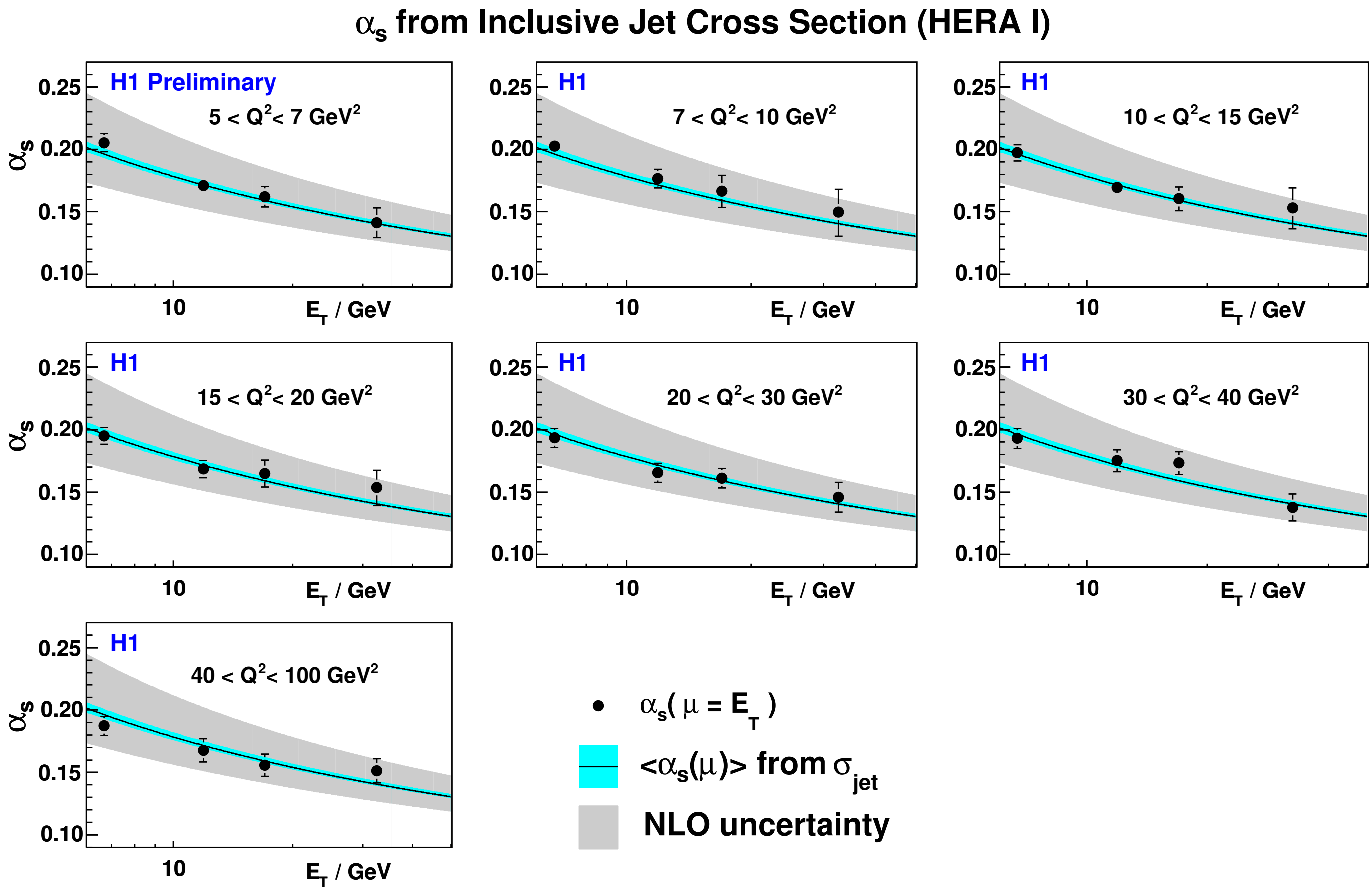

Figure 7: Results of the fitted values of $\alpha_s(E_T)$ using the inclusive jet cross sections for seven regions of Q^2. The error bar denotes the total experimental uncertainty of each data point. The solid line shows the two loop solution of the renormalisation group equation evolving the $\alpha_s(M_Z)$ obtained from a fit of 28 measurements of double differential inclusive jet cross sections $d^2\sigma/dQ^2dE_T$ (Fig.5), with the inner blue band denoting the correlated experimental uncertainties and the grey band denoting the theoretical uncertainties associated with the renormalisation and factorisation scales, PDF uncertainty and the hadronisation corrections.

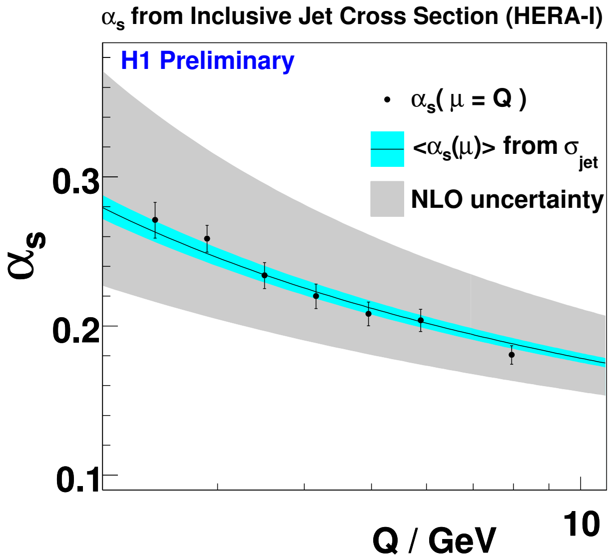

Figure 8: Results of the fitted values of $\alpha_s(\mu = Q)$ averaged over all E_T regions. The error bar denotes the total experimental uncertainty of each data point. The solid line shows the two loop solution of the renormalisation group equation evolving the $\alpha_s(M_Z)$ obtained from a fit of 28 measurements of double differential inclusive jet cross sections $d^2\sigma/dQ^2dE_T$ (Fig.5), with the inner blue band denoting the correlated experimental uncertainties and the grey band denoting the theoretical uncertainties associated with the renormalisation and factorisation scales, PDF uncertainty and the hadronisation corrections.

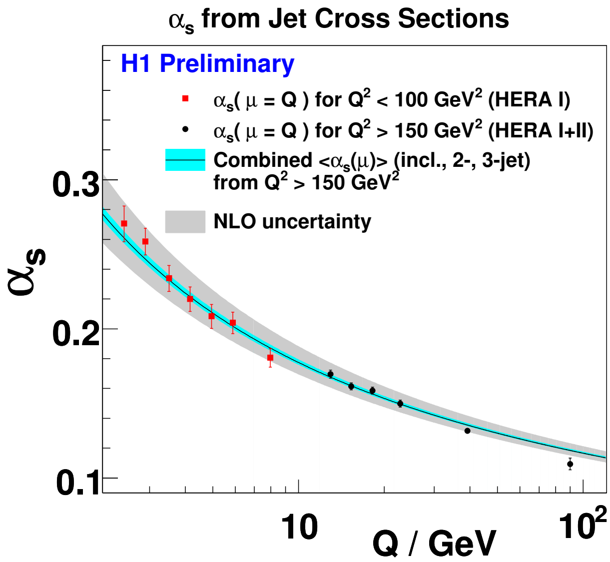

Figure 9: Results of the fitted values of $\alpha_s(\mu = Q)$ from the low Q^2 measurements (red points, same as poins on Fig.8) and the high Q^2 measurements (black points, H1prelim-08-031). The error bar denotes the total experimental uncertainty of each data point. The solid curve shows the result of evolving $\alpha_s(M_Z)$ obtained from a fit to the inclusive, dijet and threejet normalised cross sections at high Q^2 ($Q^2 > 150\ GeV^2$), with the inner blue band denoting the correlated experimental uncertainties and the grey band denoting the theoretical uncertainties associated with the renormalisation and factorisation scales, PDF uncertainty and the hadronisation corrections.